Chapter 18
Cyclical Parthenogenesis Optimization Algorithm

18.1 Introduction

Over the last few decades, metaheuristic algorithms have been successfully used for solving complex global optimization problems in science and engineering. These methods, which are usually inspired by natural phenomena, do not require any gradient information of the involved functions and are generally independent of the quality of the starting points. As a result, metaheuristic optimizers are favorable choices when dealing with discontinuous, multimodal, non-smooth, and non-convex functions, especially when near-global optimum solutions are sought, and the intended computational effort is limited.

Different characteristics of these algorithms cause them to perform dissimilarly on different classes of optimization problems, and therefore none of them can defeat all the others on all cases. As an everlasting source of inspiration, nature continues to provide researchers with different ideas in their search for new efficient optimization algorithms.

In the present chapter, a new metaheuristic algorithm is presented based on the reproduction and social behavior of some zoological species like aphids [1]. Aphids, which are considered as a highly successful group of organisms from a zoological standpoint [2], can switch between sexual and asexual reproduction mechanisms. In favorable circumstances, parthenogenesis and telescoping of generations enable aphids to achieve very high rates of reproduction [3]. This enables the aphids to exploit advantageous environmental conditions like abundance of food. However, probably to maintain genetic diversity and in response to adverse changes in environmental situation, female aphids reproduce sexual females and males when they find it necessary. Although the reasons behind reproduction behavior of aphids are not completely agreed upon in zoology, advantages of both of these alternating systems are evident from an optimization point of view.

The remainder of this chapter is organized as follows. In Sect. 18.2, the new optimization algorithm is presented subsequent to a concise and simplified

A. Kaveh, *Advances in Metaheuristic Algorithms for Optimal Design of Structures*,
DOI 10.1007/978-3-319-46173-1_18

introduction to real aphids. Sensitivity of CPA to its parameters is studied in Sect. 18.3. Some mathematical and engineering design benchmark problems are then studied in Sect. 18.4 in order to examine the efficiency of the proposed algorithm. The concluding remarks are finally presented in Sect. 18.5.

18.2 Cyclical Parthenogenesis Algorithm

In this section cyclical parthenogenesis algorithm (CPA) is introduced and described as a population-based metaheuristic algorithm for global optimization. The main rules of CPA are explained using some key aspects of the lives of aphids as a highly successful organism. Not all the details of the complicated life cycles of about 4000 species of aphids are known to us; however, there are some common features of these intricate life cycles such as the ability to reproduce both sexually and asexually (cyclical parthenogenesis), which seem to be interesting from an optimization point of view.

18.2.1 Aphids and Cyclical Parthenogenesis

Aphids are small sap-sucking insects, and members of the superfamily Aphidoidea [4]. As one of the most destructive insect pests on cultivated plants in temperate regions, aphids have fascinated and frustrated man for a very long time. This is mainly because of their intricate life cycles and close association with their host plants and their ability to reproduce both asexually and sexually [3]. Figure 18.1 shows a female aphid surrounded by her offspring on a host plant.

Aphids are capable of reproducing offspring both sexually and asexually. In asexual reproduction the offspring arise from the female parent and inherit the genes of that parent only. In asexual reproduction most of the offspring are genetically identical to their mother and genetic changes occur relatively rarely [3]. This form of reproduction is chosen by female aphids in suitable and stable environments and allows them to rapidly grow a population of similar aphids, which can exploit the favorable circumstances. Sexual reproduction, on the other hand, offers a net advantage by allowing more rapid generation of genetic diversity, making adaptation to changing environments available [5].

Since the habitat occupied by an aphid species is not uniform but consists of a spatial–temporal mosaic of many different patches, each with its own complement of organisms and resources [3], aphids employ sexual reproduction in order to maintain the genetic diversity required for increasing the chance of including the fittest genotype for a particular patch. This is the basis of the lottery model proposed by Williams [6] for explaining the role of sexual reproduction in evolution.

Some aphid species produce winged offspring in response to poor conditions on the host plant or when the population on the plant becomes too large. These winged

Fig. 18.1 A female aphid surrounded by her offspring on a host plant

offspring, which are called alates, can disperse to other food sources [4]. Flying aphids have little control over the direction of their flight because of their low speed. However, once within the layer of relatively still air around vegetation, aphids can control their landing on plants and respond to either olfactory or visual cues, or both.

18.2.2 Description of Cyclical Parthenogenesis Algorithm

Cyclical Parthenogenesis Algorithm (CPA) is a population-based metaheuristic optimization algorithm inspired from social and reproduction behavior of aphids. It starts with a population of randomly generated candidate solutions metaphorized as aphids. The quality of the candidate solutions is then improved using some simplified rules inspired from the life cycle of aphids.

Naturally, CPA does not attempt to represent an exact model of the life cycle of aphids, which is neither possible nor necessary. Instead, it encompasses certain features of their behavior to construct a global optimization algorithm.

Like many other population-based metaheuristic algorithms, CPA starts with a population of N_a candidate solutions randomly generated in the search space. These candidate solutions, which are considered as aphids, are grouped into N_c colonies, each inhabiting a host plant. These aphids reproduce offspring through sexual and asexual reproduction mechanisms. Like real aphids, in general, larger (fitter) individuals within a colony have a greater reproductive potential than smaller

ones. Some of the aphids prefer to leave their current host plant and search for better conditions. In CPA it is assumed that these flying aphids cannot fly much further due to their weak wings and end up on a plant occupied by another colony nearby. Like real aphids, the agents of the algorithm can reproduce for multiple generations. However, the life span of aphids is naturally limited, and less fit ones are more likely to be dead in adverse circumstance. The main steps of CPA can be stated as follows:

Step 1: Initialization
A population of N_a initial solutions is generated randomly:

$$x_{ij}^0 = x_{j,\min} + rand\left(x_{j,\max} - x_{j,\min}\right) \qquad j = 1, 2, \ldots, n \tag{18.1}$$

where x_{ij}^0 is the initial value of the jth variable of the ith candidate solution; $x_{j,\max}$ and $x_{j,\min}$ are the maximum and minimum permissible values for the jth variable, respectively; *rand* is a random number from a uniform distribution in the interval [0, 1]; and n is the number of optimization variables. The candidate solutions are then grouped into N_c colonies, each inhabiting a host plant. The number of aphids in all colonies N_m is equal.

Step 2: Evaluation, Reproduction, and Flying
The objective function values for the candidate solutions are evaluated. The aphids on each plant are sorted in the ascending order of their objective function values and saved in a female memory (FM). Each of the members of the female memory is capable of asexually reproducing a genetically identical clone in the next iteration.

In each iteration, N_m new candidate solutions are generated in each of the colonies in addition to identical clones. These new solutions can be reproduced either sexually or asexually. A ratio F_r of the best of these new solutions is considered as female aphids; the rest are considered as male aphids.

Asexually Generated New Solutions
A female parent is selected randomly from the population of all female parents of the colony (identical clones and newly produced females). Then, this female parent reproduces a new offspring asexually by the following expression:

$$x_{ij}^{k+1} = F_j^k + \alpha_1 \times \frac{randn}{k} \times \left(x_{j,\max} - x_{j,\min}\right) \qquad j = 1, 2, \ldots, n \tag{18.2}$$

where x_{ij}^{k+1} is the value of the jth variable of the ith candidate solution in the *(k + 1)* th iteration; F_j^k is the value of the corresponding variable of the female parent in the kth iteration; *randn* is a random number drawn from a normal distribution; and α_1 is a scaling parameter.

Sexually Generated New Solutions
Each of the male aphids selects a female randomly in order to produce an offspring sexually:

$$x_{ij}^{k+1} = M_j^k + \alpha_2 \times rand \times \left(F_j^k - M_j^k\right) \qquad j = 1, 2, \ldots, n \tag{18.3}$$

where M_j^k is the value of the jth variable of the male solution in the kth iteration and α_2 is a scaling factor. It can be seen that in a sexual reproduction, two different solutions share information, while in an asexual reproduction, the new solution is generated using merely the information of one single parent solution.

Death and Flight
When all of the new solutions of all colonies are generated, flying occurs with a probability of P_f where two of the colonies are selected randomly and a winged aphid asexually reproduced by and identical to the best female of Colony1 flies to Colony2. In order to keep the number of members of each colony constant, it is assumed that the worst member of Colony2 dies.

Step 3: Updating the Colonies
The objective function values of the newly generated candidate solutions are evaluated and the female memories are updated.

Step 4: Termination
Steps 2 and 3 are repeated until a termination criterion is satisfied. The pseudo code of CPA is presented in Table 18.1.

18.3 Sensitivity Analysis of CPA

Performance of a metaheuristic algorithm is highly dependent on the values of its internal parameters. In this section, the sensitivity of CPA to its parameters is investigated considering the weight minimization of a 10-bar truss, as depicted in Fig. 18.2. The details of this problem are further explained in the next section. A parametric study is performed considering N_a, N_c, F_r, P_f, α_1, and α_2. In each case, the problem is solved ten times in order to obtain statistically significant results. The total number of structural analyses is set as 24,000. The results of the sensitivity analysis of CPA for this example are provided in Table 18.2. When studying each parameter, the other parameters are kept unchanged. The initial values of parameters to be used in the sensitivity analysis process are $N_a = 60$, $N_c = 4$, $F_r = 0.4$, $\alpha_1 = 1$, and $\alpha_2 = 2$. A linear function increasing from 0 to 1 is considered for P_f.

A diversity index as introduced by Kaveh and Zolghadr [7] is also used to study the exploration/exploitation behavior of the algorithm for different parameter values. The index reflects the relative positions of the agents of an algorithm and can be used to observe the diversity of the agents of an algorithm during an optimization process:

Table 18.1 Pseudo code of the CPA algorithm [1]

procedure Cyclical Parthenogenesis Algorithm
begin
Initialize parameters**;**
Initialize a population of N_a random candidate solutions;
Group the candidate solutions in N_c colonies with each having N_m members;
Evaluate and Sort the candidate solutions of each colony and save the best N_m ones in Female Memory

while (termination condition not met) **do**
for m: 1 to N_c
Reproduce an identical solution by each of the solutions of the Female Memory
Divide the newly generated offspring into male and female considering F_r
for i: 1 to $F_r \times N_m$
Generate new solution *i* asexually using Eq. (18.2)
end for
for i: $F_r \times N_m + 1$ to N_m
Generate new solution *i* sexually using Eq. (18.3)
end for
if rand$<P_f$
Select two colonies randomly
Generate an winged identical offspring from the best solution of Colony1
Eliminate the worst solution of Colony2 and move winged aphid to Colony2
end if
Evaluate the objective function values of new aphids
Update the Female Memory
end for
end while
end

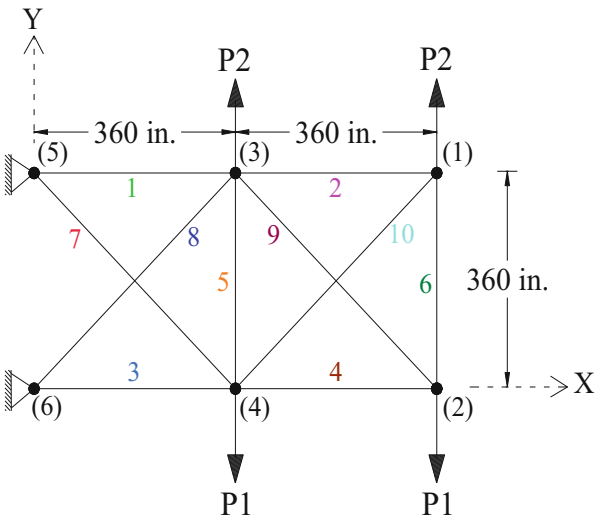

Fig. 18.2 Schematic of the planar 10-bar truss structure

$$Diversity\ \ Index = \frac{1}{nP}\sum_{j=1}^{nP}\sqrt{\sum_{i=1}^{nVAR}\left(\frac{GB(i)-X_j(i)}{X_{i,\max}-X_{i,\min}}\right)^2} \tag{18.4}$$

where $X_j(i)$ is the value of the ith variable of the jth particle; $X_{i,\min}$ and $X_{i,\max}$ are the minimum and maximum values of the ith variable, respectively; $nVAR$ is the number of design variables; and nP is the number of particles. In order to decrease random fluctuations, the mean values of diversity index in the ten independent runs are plotted against iteration numbers for each parameter set.

In order to study the effect of population size (N_a), the algorithm is run with 20, 40, 60, 80, and 100 aphids, while keeping the total number of structural analyses unchanged. From Table 18.2 it can be seen that the best performance of CPA in terms of the best weight, mean weight, and standard deviation is obtained for $N_a = 60$. The second best results are obtained when considering $N_a = 80$. The best and mean performance of the algorithm for different values of N_a is depicted in Fig. 18.3.

The concept of multiple colonies allows CPA to search different portions of the search spaces more or less independently and prevents the unwanted premature convergence phenomenon. Table 18.2 shows the statistical information for different values of N_c, i.e., the number of colonies, where the population size is kept unchanged ($N_a = 60$). As it can be seen, the best performance in terms of best weight, mean weight, and standard deviation is obtained for $N_c = 4$. This parameter value provides a good balance between the diversification and intensification tendencies of the algorithm. In fact, dividing the population of aphids into more colonies limits the circulation of information among the aphids and allows the aphids of a colony to explore the search space more independently without being affected by other colonies. This generally results in a more diverse search. On the

Table 18.2 Results of the sensitivity analysis of CPA for the 10-bar truss

Parameter/value	Best weight (lb)	Mean weight (lb)	Standard deviation (lb)
Population size			
Na = 20	5062.89	5074.42	8.61
Na = 40	5061.11	5063.68	5.18
Na = 60	5060.94	5061.35	0.23
Na = 80	5061.08	5061.50	0.51
Na = 100	5061.17	5061.98	0.53
Number of colonies			
Nc = 1	5061.01	5064.76	6.42
Nc = 2	5061.15	5062.01	2.04
Nc = 3	5061.04	5062.97	4.98
Nc = 4	5060.94	5061.35	0.23
Nc = 6	5061.24	5062.10	0.65
Nc = 12	5061.89	5067.62	7.05
Female ratio			
Fr = 0.2	5060.98	5061.49	0.53
Fr = 0.4	5060.94	5061.35	0.23
Fr = 0.6	5061.06	5061.76	0.59
Fr = 0.8	5061.64	5067.59	7.54
Flight probability			
Pf = 1	5061.04	5063.34	4.98
Pf = 0	5061.06	5062.89	2.90
Pf linear	5060.94	5061.35	0.23
Step size			
α_1 =0.5 and α_2 =0.5	5314.20	5785.27	35.50
α_1 = 0.5 and α_2 = 1	5169.72	5684.86	223.67
α_1 = 0.5 and α_2 = 2	5061.03	5061.90	0.59
α_1 = 1 and α_2 = 0.5	5100.97	5301.86	149.41
α_1 = 1 and α_2 = 1	5084.95	5410.06	235.75
α_1 = 1 and α_2 = 2	5060.94	5061.35	0.23
α_1 = 2 and α_2 = 0.5	5085.01	5165.37	111.6
α_1 = 2 and α_2 = 1	5062.51	5088.97	35.51
α_1 = 2 and α_2 = 2	5061.04	5062.97	4.85
α_1 = 2 and α_2 = 4	5062.06	5073.81	6.37
α_1 = 4 and α_2 = 2	5061.61	5065.18	6.63
α_1 = 4 and α_2 = 4	5062.23	5069.80	7.84

other hand, having more aphids in a colony (less number of colonies) permits the algorithm to search a particular region of the search space more thoroughly (more intensification), but, at the same time, limits the diversification of the algorithm. The best and mean performance of the algorithm for different values of N_c is depicted in Fig. 18.4. The diversity index curves of CPA for different values of N_c are shown in Fig. 18.5. It can be seen that the curves corresponding to $N_c = 3$ and $N_c = 4$, which result in the best performance of the algorithm, are placed between

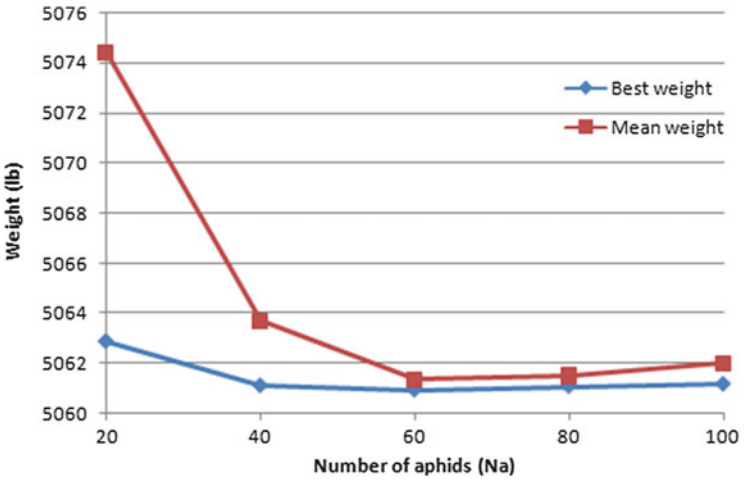

Fig. 18.3 Best and mean performance of CPA for different values of N_a

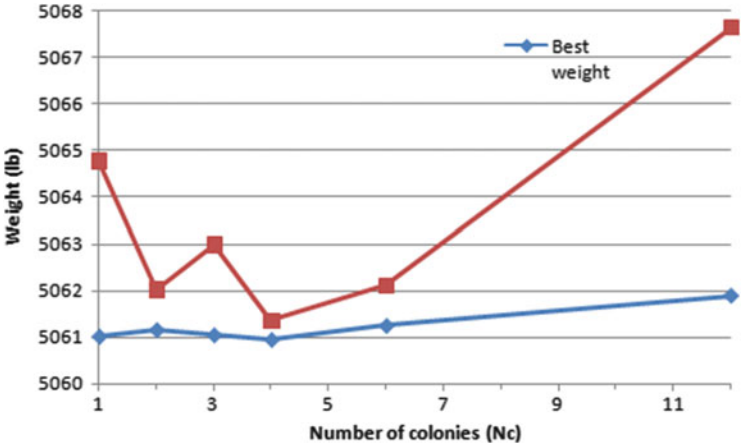

Fig. 18.4 Best and mean performance of CPA for different values of N_c

those of $N_c = 1$ and $N_c = 2$ from below and $N_c = 6$ and $N_c = 12$ from above. This conforms to the above discussion, i.e., dividing the aphids into more colonies generally results in slower rate of convergence (more diversity index values). $N_c = 4$ seems to provide a good balance between the exploration and exploitation tendencies of the algorithm.

Parameter F_r defines the ratio of female aphids to all of the newly generated aphids. Increasing the value of this parameter results in an increase in the number of asexually generated aphids of the next generation. Since such aphids use a single source of information (female parent), they can be interpreted as means of searching a localized region around their parent. This localized region gets smaller gradually as the optimization process proceeds. Sexual reproduction, on the other

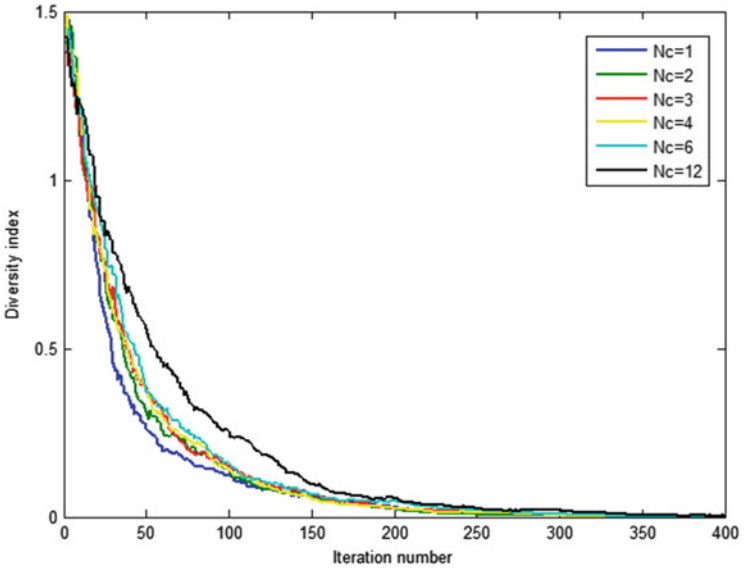

Fig. 18.5 Diversity index curves of CPA for different values of N_c

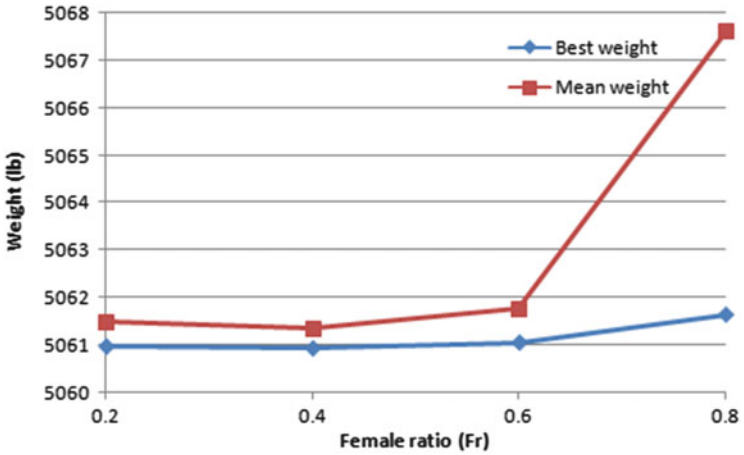

Fig. 18.6 Best and mean performance of CPA for different values of F_r

hand, incorporates two different sources of information and therefore contributes to the convergence of the algorithm by letting the aphids share information. According to Table 18.2 which summarizes the statistical information for different values of F_r, it can be seen that the proposed algorithm exhibits its best performance in terms of mean weight when the value of this parameter is taken as 0.4, while the second and third best performances are obtained for $F_r = 0.2$ and $F_r = 0.6$. The best and mean performance of the algorithm for different values of N_a is depicted in Fig. 18.6. The diversity index curves of CPA for different values of F_r are shown

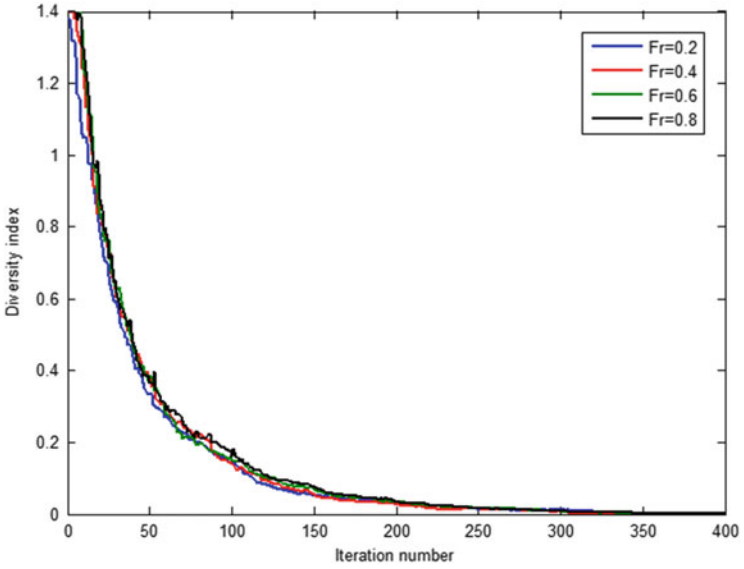

Fig. 18.7 Diversity index curves of CPA for different values of F_r

in Fig. 18.7. It can be seen that increasing the value of F_r slightly increases the diversity of the aphids in the search space, i.e., the curves corresponding to $F_r = 0.8$ and $F_r = 0.2$ are placed above and below the other curves, respectively. However, the effect is not very significant and the curves are very close to each other.

Parameter P_f is responsible for defining the level of information exchange among the colonies. With no possible flights, the colonies would be performing their search in a completely independent manner, i.e., an optimization run with N_a aphids divided into four colonies would be similar to four independent runs each with $N_a/4$ aphids per colony. It is obvious that this would not be particularly favorable, since it is in fact changing the population of aphids without actually utilizing the abovementioned benefits of multiple colonies. On the other hand, permitting too many flights results corresponds to merging the information sources of different colonies. It is important to note that at the early stages of the optimization process, it is more favorable to give the colonies a higher level of independence so that they can search the problem space without being affected by the other colonies. However, as the optimization process proceeds, it is desirable to let the colonies share more information so as to provide the opportunity for the more promising regions of the search space to be searched more thoroughly. Three different cases are considered for P_f in this study: $P_f = 0$, $P_f = 1$, and P_f linearly increasing from 0 to 1. It can be clearly seen from Table 18.2 that the best performance of the algorithm corresponds to the linear case, since it conforms to the abovementioned discussion on information circulation. The diversity index curves of CPA for different values of P_f are shown in Fig. 18.8. It can be seen

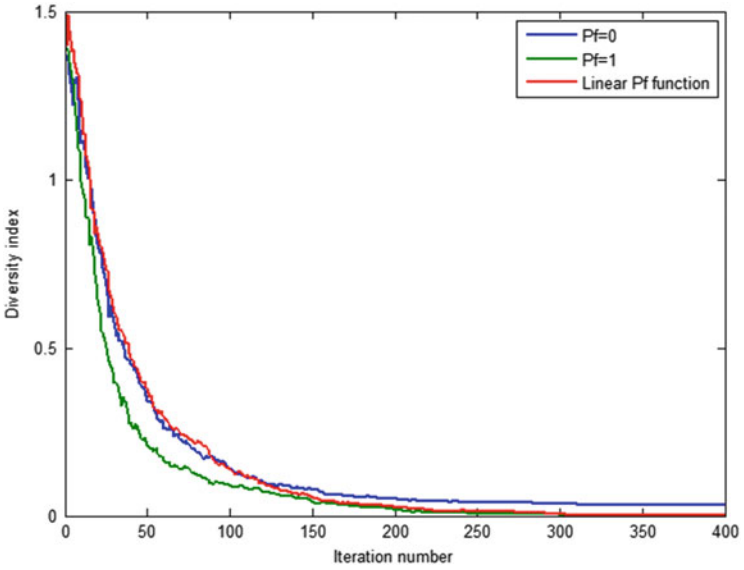

Fig. 18.8 Diversity index curves of CPA for different values of P_f

that when $P_f = 0$, the diversity index values are relatively high even at the end of the optimization process. This means that the different colonies have converged to different results. The curve corresponding to the linear function is similar to that of $P_f = 0$ at the early stages of the optimization process, while it gets closer to the curve corresponding to $P_f = 1$ at the final stages. This explains the favorable behavior of the algorithm when a linear function is chosen for P_f.

Parameters α_1 and α_2 represent the step size of the agents in asexual and sexual reproductions, respectively. The sensitivity of CPA to these two parameters is also shown in Table 18.2. The diversity index curves of CPA for different values of α_1 and α_2 are shown in Fig. 18.9. According to Table 18.2 the best performance of the algorithm corresponds to $\alpha_1 = 1$ and $\alpha_2 = 2$. There are two other cases which result in relatively good performance of the algorithm, i.e., $\alpha_1 = 0.5$ and $\alpha_2 = 2$ and $\alpha_1 = 2$ and $\alpha_2 = 2$. As it can be seen in Fig. 18.9, the diversity index curves for these three cases are almost the same.

18.4 Test Problems and Optimization Results

In order to evaluate the efficiency of the proposed algorithm, some benchmark test problems are considered from the literature. A set of unimodal and multimodal mathematical optimization problems are studied in Sect. 18.4.1. In addition, truss weight minimizations of a planar 10-bar truss, a spatial 25-bar transmission tower, a spatial 72-bar truss, a 120-bar dome-shaped truss, and a planar 200-bar truss are

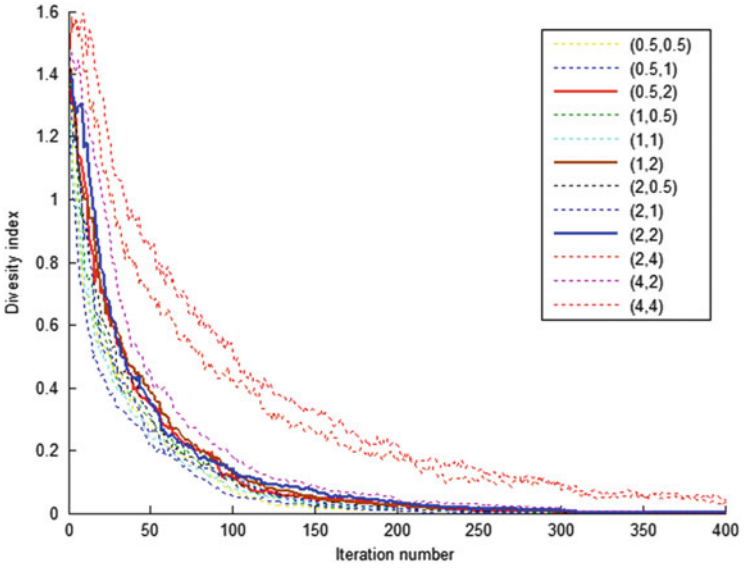

Fig. 18.9 Diversity index curves of CPA for different values of *Alpha1*, *Alpha2*

considered as structural optimization problems. The results of utilizing CPA on these structural optimization problems are then compared to some of the state-of-the-art metaheuristic algorithms.

18.4.1 Mathematical Optimization Problems

In this section, the efficiency of the CPA is evaluated by solving the mathematical benchmark problems summarized in Table 18.3. These benchmark problems are taken from Ref. [8], where some variants of GA were used as the optimization algorithm. The results obtained by CPA are presented in Table 18.4 along with those of some GA variants. Each objective function is optimized 50 times independently starting from different initial populations, and the average number of function evaluations required by each algorithm is presented. The numbers in the parentheses indicate the ratio of the successful runs in which the algorithm has obtained the global minimum with predefined accuracy, which is taken as $\varepsilon = f_{\min} - f_{final} = 10^{-4}$. The absence of the parentheses indicates that the algorithm has been successful in all independent runs.

As it can be seen from Table 18.4, CPA generally performs better than GA and its variants in the mathematical optimization problems considered in this study.

Table 18.3 Details of the benchmark mathematical problems solved in this study

Function name	Side constraints	Function	Global minimum
Aluffi-Pentini	$\mathbf{X} \in [-10,10]^2$	$f(\mathbf{X}) = \frac{1}{4}x_1^4 - \frac{1}{2}x_1^2 + \frac{1}{10}x_1 + \frac{1}{2}x_2^2$	*−0.352386*
Bohachevsky 1	$\mathbf{X} \in [-100,100]^2$	$f(\mathbf{X}) = x_1^2 + 2x_2^2 - \frac{3}{10}\cos(3\pi x_1) - \frac{4}{10}\cos(4\pi x_2) + \frac{7}{10}$	*0.0*
Bohachevsky 2	$\mathbf{X} \in [-50,50]^2$	$f(\mathbf{X}) = x_1^2 + 2x_2^2 - \frac{3}{10}\cos(3\pi x_1)\cos(4\pi x_2) + \frac{3}{10}$	*0.0*
Becker and Lago	$\mathbf{X} \in [-10,10]^2$	$f(\mathbf{X}) = \left(\lvert x_1\rvert - 5\right)^2 + \left(\lvert x_2\rvert - 5\right)^2$	*0.0*
Branin	$0 \le x_2 \le 15\ -5 \le x_1 \le 10$	$f(\mathbf{X}) = \left(x_2 - \frac{5.1}{4\pi^2}x_1^2 + \frac{5}{\pi}x_1\right)^2 + 10\left(1 - \frac{1}{8\pi}\right)\cos(x_1) + 10$	*0.397887*
Camel	$\mathbf{X} \in [-5,5]^2$	$f(\mathbf{X}) = 4x_1^2 - 2.1x_1^4 + \frac{1}{3}x_1^6 + x_1x_2 - 4x_2^2 + 4x_2^4$	*−1.0316*
Cb3	$\mathbf{X} \in [-5,5]^2$	$f(\mathbf{X}) = 2x_1^2 - 1.05x_1^4 + \frac{1}{6}x_1^6 + x_1x_2 + x_2^2$	*0.0*
Cosine mixture	$n = 4, \mathbf{X} \in [-1,1]^n$	$f(\mathbf{X}) = \sum_{i=1}^{n} x_i^2 - \frac{1}{10}\sum_{i=1}^{n}\cos(5\pi x_i)$	*−0.4*
DeJoung	$\mathbf{X} \in [-5.12,5.12]^3$	$f(\mathbf{X}) = x_1^2 + x_2^2 + x_3^2$	*0.0*
Exponential	$n = 2,4,8, \mathbf{X} \in [-1,1]^n$	$f(\mathbf{X}) = -\exp\left(-0.5\sum_{i=1}^{n} x_i^2\right)$	*−1*
Goldstein and Price	$\mathbf{X} \in [-2,2]^2$	$f(\mathbf{X}) = \left[1 + (x_1 + x_2 + 1)^2\left(19 - 14x_1 + 3x_1^2 - {}^1 14x_2 + 6x_1x_2 + 3x_2^2\right]\right.$ $\left.\times\left[30 + (2x_1 - 3x_2)^2\left(18 - 32x_1 + 12x_1^2 + 48x_2 - 36x_1x_2 + 27x_2^2\right]^2\right.\right.$	*3.0*
Griewank	$\mathbf{X} \in [-100,100]^2$	$f(\mathbf{X}) = 1 + \frac{1}{200}\sum_{i=1}^{2} x_i^2 - \prod_{i=1}^{2}\cos\left(\frac{x_i}{\sqrt{i}}\right)$	*0.0*
Hartman 3	$\mathbf{X} \in [0,1]^3$	$f(\mathbf{X}) = -\sum_{i=1}^{4} c_i \exp\left(-\sum_{j=1}^{3} a_{ij}\left(x_j - p_{ij}\right)^2\right)$ $a = \begin{bmatrix} 3 & 10 & 30 \\ 0.1 & 10 & 35 \\ 3 & 10 & 30 \\ 0.1 & 10 & 35 \end{bmatrix}$, $c = \begin{bmatrix} 1 \\ 1.2 \\ 3 \\ 3.2 \end{bmatrix}$, *and* $p = \begin{bmatrix} 0.3689 & 0.117 & 0.2673 \\ 0.4699 & 0.4387 & 0.747 \\ 0.1091 & 0.8732 & 0.5547 \\ 0.03815 & 0.5743 & 0.8828 \end{bmatrix}$.	*−3.862782*

Hartman 6	$\mathbf{X} \in [0,1]^6$	$f(\mathbf{X}) = -\sum_{i=1}^{4} c_i \exp\left(-\sum_{j=1}^{6} a_{ij}\left(x_j - p_{ij}\right)^2\right)$ $a = \begin{bmatrix} 10 & 3 & 17 & 3.5 & 1.7 & 8 \\ 0.05 & 10 & 17 & 0.1 & 8 & 14 \\ 3 & 3.5 & 17 & 10 & 17 & 8 \\ 17 & 8 & 0.05 & 10 & 0.1 & 14 \end{bmatrix}$, $c = \begin{bmatrix} 1 \\ 1.2 \\ 3 \\ 3.2 \end{bmatrix}$, *and* $p = \begin{bmatrix} 0.1312 & 0.1696 & 0.5569 & 0.0124 & 0.8283 & 0.5886 \\ 0.2329 & 0.4135 & 0.8307 & 0.3736 & 0.1004 & 0.9991 \\ 0.2348 & 0.1451 & 0.3522 & 0.2883 & 0.3047 & 0.6650 \\ 0.4047 & 0.8828 & 0.8732 & 0.5743 & 0.1091 & 0.0381 \end{bmatrix}$	-3.322368

Table 18.4 Performance comparison of CPA and some GA variants in the mathematical optimization problems

Function name	GEN	GEN–S	GEN–S–M	GEN–S–M–LS	CPA
AP	1360 (0.99)	1360	1277	1253	560
Bf1	3992	3356	1640	1615	1173
Bf2	20,234	3373	1676	1636	1376
BL	19,596	2412	2439	1436	424
Branin	1442	1418	1404	1257	708
Camel	1358	1358	1336	1300	482
Cb3	9771	2045	1163	1118	548
CM	2105	2105	1743	1539	1612
DeJoung	9900	3040	1462	1281	670
Exp2	938	936	817	807	435
Exp4	3237	3237	2054	1496	781
Exp8	3237	3237	2054	1496	1105
Goldstein and Price	1478	1478	1408	1325	805
Griewank	18,838 (0.91)	3111 (0.91)	1764	1652 (0.99)	1572
Hartman 3	1350	1350	1332	1274	1128
Hartman 6	2562 (0.54)	2562 (0.54)	2530 (0.67)	1865 (0.68)	1533

18.4.2 Truss Design Problems

In order to further investigate the efficiency of the CPA, five continuous truss design problems are considered in this section. The results are compared to those obtained by some of the state-of-the-art metaheuristic optimization algorithms. 60 aphids are considered for all of the benchmark truss optimization problems. The total number of iterations is considered as 400 for all of the examples except for the last one, where 600 iterations are permitted. These constrained optimization problems are turned into unconstrained ones using a penalty approach. If the constraints are satisfied, then the amount of penalty will be zero; otherwise its value can be calculated as the ratio of violated constraint to the corresponding allowable limit. The CPA is coded in the MATLAB software environment. The required structural analyses are carried out using the direct stiffness method also coded in MATLAB.

18.4.2.1 Design of a Planar 10-Bar Truss Structure

A 10-bar truss as shown in Fig. 18.2 is considered as the first structural design problem. This is a well-known problem in the field of structural optimization and has been solved by many researchers using different optimization algorithms. The material density is 0.1 lb/in^3 and the modulus of elasticity is 10,000 ksi. The members are subjected to stress limitation of 25 ksi, while the horizontal and vertical displacements of all nodes are limited to $\pm$ 2.0 in. Each of the members is

Table 18.5 Optimized results obtained by CPA and some other metaheuristic algorithms for the 10-bar truss problem

	Optimal cross-sectional areas (in^2)					
Element group	ABC-AP [9]	SAHS [10]	TLBO [11]	MSPSO [12]	WEO [13]	Present work
Case 1						
1	30.5480	30.3940	30.4286	30.5257	30.5755	30.5022
2	0.1000	0.1000	0.1000	0.1001	0.1000	0.1000
3	23.1800	23.0980	23.2436	23.2250	23.3368	23.2170
4	15.2180	15.4910	15.3677	15.4114	15.1497	15.2204
5	0.1000	0.1000	0.1000	0.1001	0.1000	0.1001
6	0.5510	0.5290	0.5751	0.5583	0.5276	0.5587
7	7.4630	7.4880	7.4404	7.4395	7.4458	7.4548
8	21.0580	21.1890	20.9665	20.9172	20.9892	21.0371
9	21.5010	21.3420	21.5330	21.5098	21.5236	21.5295
10	0.1000	0.1000	0.1000	0.1000	0.1000	0.1002
Best weight (lb)	5060.880	5061.42	5060.96	5061	5060.99	5060.92
Mean weight (lb)	N/A	5061.95	5062.08	5064.46	5062.09	5062.45
Standard dev. (lb)	N/A	0.71	0.79	5.72	2.05	3.77
No. structural analyses	500×10^3	7081	16,872	N/A	19,540	23700
Case 2						
1	23.4692	23.5250	23.5240	23.4432	23.5804	23.5515
2	0.1005	0.1000	0.1000	0.1000	0.1003	0.1000
3	25.2393	25.4290	25.4410	25.3718	25.1582	25.5440
4	14.3540	14.4880	14.4790	14.1360	14.1801	14.1674
5	0.1001	0.1000	0.1000	0.1000	0.1002	0.1000
6	1.9701	1.9920	1.9950	1.9699	1.9708	1.9698
7	12.4128	12.3520	12.3340	12.4335	12.4511	12.3533
8	12.8925	12.6980	12.6890	13.0173	12.9349	12.8167
9	20.3343	20.3410	20.3540	20.2717	20.3595	20.3302
10	0.1000	0.1000	0.1000	0.1000	0.1001	0.1001
Best weight (lb)	4677.077	4678.84	4678.31	4677.26	4677.31	4677.16
Mean weight (lb)	N/A	4680.08	4680.12	4681.45	4679.06	4678.62
Standard dev. (lb)	N/A	1.89	1.016	2.19	2.07	0.95
No. structural analyses	500×10^3	7267	14,857	N/A	19,890	23640

considered as an independent design variable with lower and upper bounds of 0.1 and 35.0 in^2, respectively. There are two independent loading cases acting on the structure: Case 1, $P_1 = 100$ kips and $P_2 = 0$, and Case 2, $P_1 = 150$ kips and $P_2 = 50$ kips.

Table 18.5 compares the optimized designs found by CPA together with some of the state-of-the-art optimization algorithms for the loading cases. It can be seen that the results found by CPA are comparable to those of the other state-of-the-art

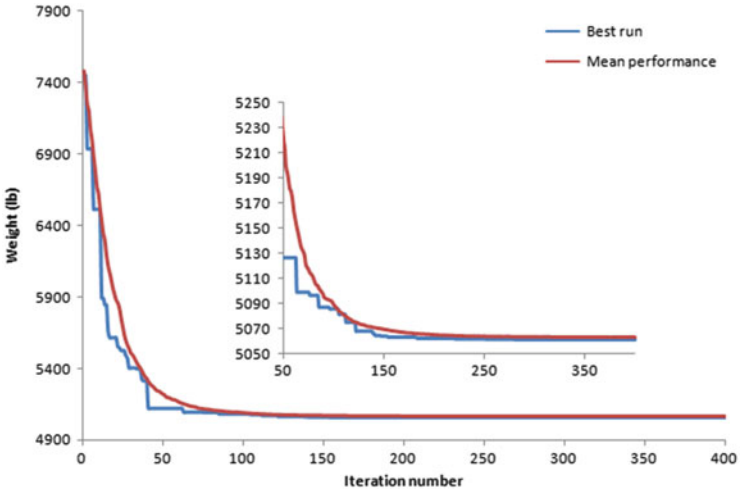

Fig. 18.10 Convergence curves of the best result of the CPA together with the mean performance of the algorithm for the 10-bar planar truss (Case 1)

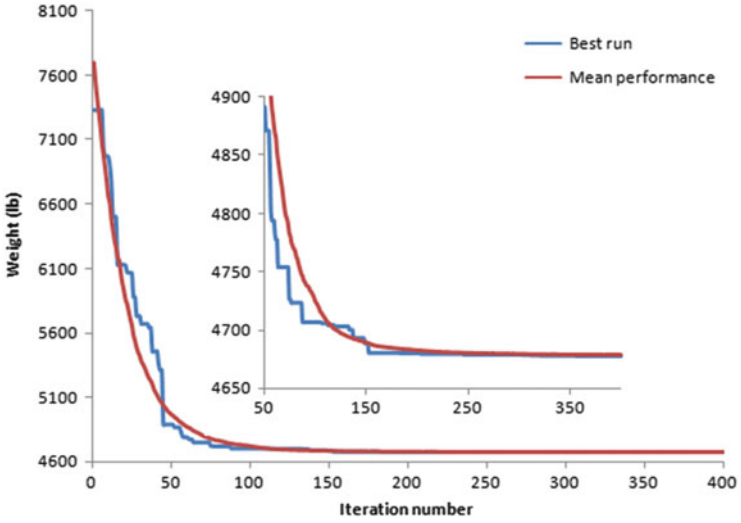

Fig. 18.11 Convergence curves of the best result of the CPA together with the mean performance of the algorithm for the 10-bar planar truss (Case 2)

algorithms. In both cases CPA has obtained the best result after that of ABC-AP. It should be noted that CPA requires less than 5 % of the structural analyses used by ABC-AP (less than 24,000 compared to 500,000). Figures 18.10 and 18.11 show the convergence curves of the best run and the mean performance of CPA on the 10-bar planar truss.

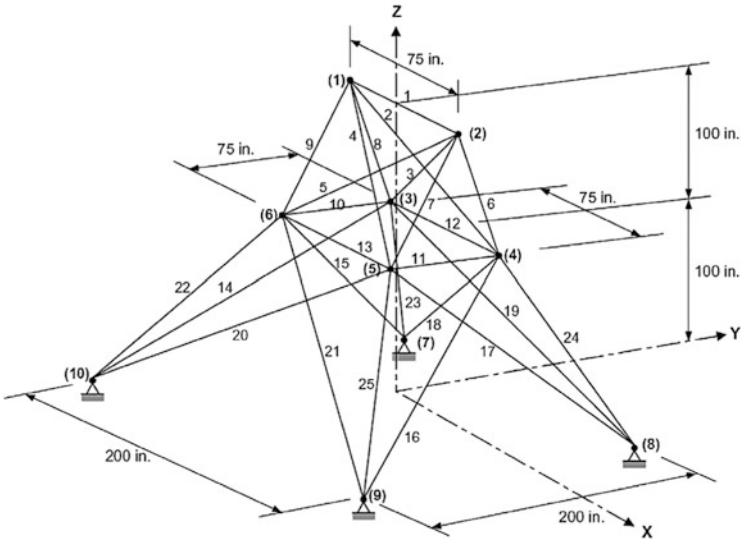

Fig. 18.12 Schematic of the spatial 25-bar transmission tower

Table 18.6 Independent loading conditions acting on the spatial 25-bar truss

	Case 1			Case 2		
Node	P_x kips	P_y kips	P_z kips	P_x kips	P_y kips	P_z kips
1	0.0	20.0	−5.0	1.0	10.0	−5.0
2	0.0	−20.0	−5.0	0.0	10.0	−5.0
3	0.0	0.0	0.0	0.5	0.0	0.0
6	0.0	0.0	0.0	0.5	0.0	0.0

18.4.2.2 Design of a 25-Bar Transmission Tower Truss

Weight minimization of a 25-bar transmission tower as schematically depicted in Fig. 18.12 is considered as the second structural optimization problem. The material density and modulus of elasticity are 0.1 lb/in^3 and 10,000 ksi, respectively.

Table 18.6 shows the two independent loading conditions applied to the structure. The 25 bars of the truss are classified into eight groups as follows:

(1) A_1, (2) A_2–A_5, (3) A_6–A_9, (4) A_{10}–A_{11}, (5) A_{12}–A_{13}, (6) A_{14}–A_{17}, (7) A_{18}–A_{21}, and (8) A_{22}–A_{25}.

Maximum displacement limitations of 0.350 in are imposed on all nodes in all directions. The axial stress constraints, which are different for each group, are shown in Table 18.7. The cross-sectional areas vary continuously from 0.01 to 3.4 in^2 for all members.

This is a very well-known test problem in the field of structural optimization and is investigated by many researchers using different optimization methods. Table 18.8 shows that the different optimization methods converged almost to the

Table 18.7 Member stress limits for the 25-bar spatial truss

Element group	Compressive stress limits ksi (MPa)	Tensile stress limits ksi (MPa)
1	35.092 (241.96)	40.0 (275.80)
2	11.590 (79.913)	40.0 (275.80)
3	17.305 (119.31)	40.0 (275.80)
4	35.092 (241.96)	40.0 (275.80)
5	35.092 (241.96)	40.0 (275.80)
6	6.759 (46.603)	40.0 (275.80)
7	6.959 (47.982)	40.0 (275.80)
8	11.082 (76.410)	40.0 (275.80)

same structural weight. Figure 18.13 shows the convergence curve of the best result of CPA together with the mean performance of the algorithm for the 25-bar spatial truss.

18.4.2.3 Design of a 72-Bar Spatial Truss

Weight optimization of a spatial 72-bar truss structure shown in Fig. 18.14 is considered as the third truss design example. The two loading conditions acting on the structure are summarized in Table 18.9. The elements are grouped to form 16 design variables according to Table 18.10. The material density and the modulus of elasticity are taken as 0.1 lb/in^3 and 10,000 ksi, respectively. All members are subjected to a stress limitation of $\pm$25 ksi. The displacements of the uppermost nodes along x- and y-axes are limited to $\pm$0.25 in. Cross-sectional areas of bars can vary between 0.10 and 4.00 in^2, respectively.

This problem has been studied by Erbatur et al. [16] using genetic algorithms, Camp and Bichon [17] using ant colony optimization, Perez and Behdinan [18] using particle swarm optimization, Camp [15] using Big Bang–Big Crunch algorithm, Kaveh and Khayatazad [19] using ray optimization, Degertekin using variants of harmony search [10], and Degertekin and Hayalioglu using teaching–learning-based optimization [11], among others.

Table 18.11 compares the results obtained by the present method to those previously reported in the literature. It can be seen that the present method have obtained the lightest design with a weight of 379.62 lb. Figure 18.15 presents the convergence curve for the best result and the mean performance of the CPA on 50 independent runs on this example.

18.4.2.4 Design of a 120-Bar Dome Truss

The fourth test problem is the weight minimization of a 120-bar dome truss shown in Fig. 18.16. This structure was considered by Soh and Yang [20] as a configuration optimization problem. It has been solved by Lee and Geem [21], Kaveh et al.

Table 18.8 Comparison of the optimization results obtained in the spatial 25-bar truss problem

		Optimal cross-sectional areas (in^2)							
		Li et al. [14]			Camp [15]	Degertekin [10]		Degertekin and Hayalioglu [11]	Present work
Element group		PSO	PSOPC	HPSO	BB–BC	EHS	SAHS	TLBO	CPA
1	A1	9.863	0.010	0.010	0.010	0.010	0.010	0.0100	0.010
2	A2–A5	1.798	1.979	1.970	2.092	1.995	2.074	2.0712	1.989
3	A6–A9	3.654	3.011	3.016	2.964	2.980	2.961	2.9570	2.988
4	A10–A11	0.100	0.100	0.010	0.010	0.010	0.010	0.0100	0.010
5	A12–A13	0.100	0.100	0.010	0.010	0.010	0.010	0.0100	0.010
6	A14–A17	0.596	0.657	0.694	0.689	0.696	0.691	0.6891	0.689
7	A18–A21	1.659	1.678	1.681	1.601	1.679	1.617	1.6209	1.678
8	A22–A25	2.612	2.693	2.643	2.686	2.652	2.674	2.6768	2.658
	Best weight (lb)	627.08	545.27	545.19	545.38	545.49	545.12	545.09	545.18
	Average weight (lb)	N/A	N/A	N/A	545.78	546.52	545.94	545.41	545.49
	Std Dev (lb)	N/A	N/A	N/A	0.491	1.05	0.91	0.42	0.24
	No. of analyses	150,000	150,000	150,000	20,566	10,391	9051	15,318	22800

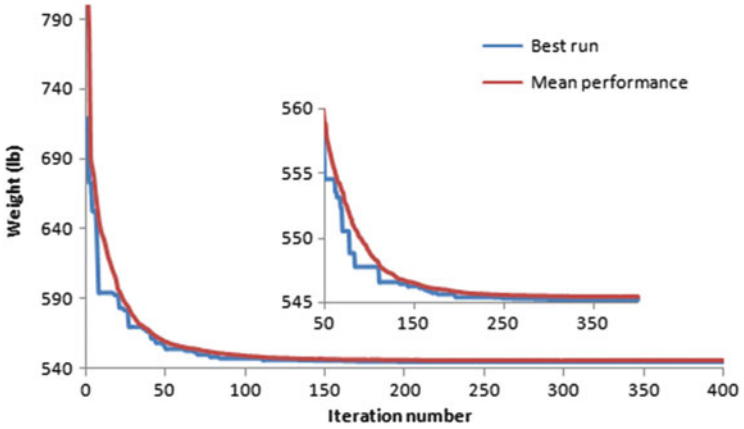

Fig. 18.13 Convergence curves of the best result of the CPA together with the mean performance of the algorithm for the 25-bar spatial truss

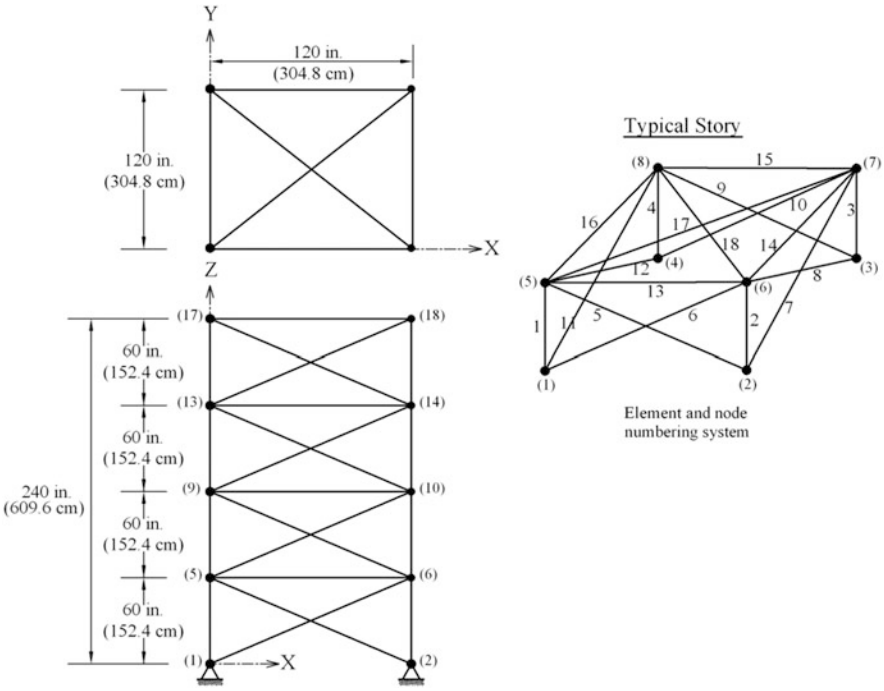

Fig. 18.14 Schematic of the spatial 72-bar truss structure

Table 18.9 Independent loading conditions acting on the spatial 72-bar truss

	Case 1			Case 2		
Node	P_x kips	P_y kips	P_z kips	P_x kips	P_y kips	P_z kips
1	5	5	−5	–	–	−5
2	–	–	–	–	–	−5
3	–	–	–	–	–	−5
4	–	–	–	–	–	−5

[22], Kaveh and Khayatazad [19], and Kaveh and Mahdavi [23] as a sizing optimization problem. The members of the structure are divided into seven groups as shown in Fig. 18.16.

The allowable tensile and compressive stresses are set according to the ASD-AISC [24] provisions as follows:

$$\begin{cases} \sigma_i^+ = 0.6F_y & for \quad \sigma_i \geq 0 \\ \sigma_i^- & for \quad \sigma_i \leq 0 \end{cases} \tag{18.5}$$

where σ_i^- is the compressive allowable stress and depends on the slenderness ratios of the elements.

$$\sigma_i^- = \begin{cases} \left[\left(1 - \dfrac{\lambda_i^2}{2{C_c}^2}\right)F_y\right] \Big/ \left(\dfrac{5}{3} + \dfrac{3\lambda_i}{8C_c} - \dfrac{\lambda_i^3}{8C_c^3}\right) & for \quad \lambda_i \leq C_c \\ \dfrac{12\pi^2 E}{23\lambda_i^2} & for \quad \lambda_i \geq C_c \end{cases} \tag{18.6}$$

where E is the modulus of elasticity, F_y is the material's yield stress, λ_i is the slenderness ratio ($\lambda_i = \frac{K_i L_i}{r_i}$), K_i is the effective length factor, L_i is the length of the member, and r_i is the radius of gyration. C_c is the critical slenderness ratio separating elastic and inelastic buckling regions $\left(C_c = \sqrt{2\pi^2 E/F_y}\right)$.

The modulus of elasticity and the material density are taken as 30,450 ksi (210 GPa) and 0.288 lb/in^3, respectively. The yield stress is taken as 58.0 ksi (400 MPa). The radius of gyration is expressed in terms of cross-sectional areas of the members as $r_i = aA_i^b$ [25]. Constants a and b depend on the types of sections adopted for the members such as pipes, angles, etc. In this example pipe sections are used for the bars for which a = 0.4993 and b = 0.6777. The dome is considered to be subjected to vertical loads at all unsupported nodes. These vertical loads are taken as −13.49 kips (60 kN) at node 1, −6.744 kips (30 kN) at nodes 2 through 14, and −2.248 kips (10 kN) at the other nodes. Four different problem variants are considered for this structure: with stress constraints and no displacement constraints (Case 1), with stress constraints and displacement limitations of ±0.1969 in (5 mm)

Table 18.10 Comparison of the optimization results obtained in the spatial 72-bar truss problem

	Optimal cross-sectional areas (in^2)								
	Erbatur et al. [16]	Camp and Bichon [17]	Perez and Behdinan [18]	Camp [15]	Kaveh and Khayatazad [19]	Degertekin [10]		Degertekin and Hayalioglu [11]	Present work
Element group	GA	ACO	PSO	BB–BC	RO	EHS	SAHS	TLBO	CPA
1–4	1.755	1.948	1.7427	1.8577	1.8365	1.967	1.860	1.9064	1.8873
5–12	0.505	0.508	0.5185	0.5059	0.5021	0.510	0.521	0.50612	0.5111
13–16	0.105	0.101	0.1000	0.1000	0.1000	0.100	0.100	0.100	0.1000
17–18	0.155	0.102	0.1000	0.1000	0.1004	0.100	0.100	0.100	0.1000
19–22	1.155	1.303	1.3079	1.2476	1.2522	1.293	1.271	1.2617	1.2554
23–30	0.585	0.511	0.5193	0.5269	0.5033	0.511	0.509	0.5111	0.5141
31–34	0.100	0.101	0.1000	0.1000	0.1002	0.100	0.100	0.100	0.1000
35–36	0.100	0.100	0.1000	0.1012	0.1001	0.100	0.100	0.100	0.1000
37–40	0.460	0.561	0.5142	0.5209	0.5730	0.499	0.485	0.5317	0.5312
41–48	0.530	0.492	0.5464	0.5172	0.5499	0.501	0.501	0.51591	0.5174
49–52	0.120	0.100	0.1000	0.1004	0.1004	0.100	0.100	0.100	0.1000
53–54	0.165	0.107	0.1095	0.1005	0.1001	0.100	0.100	0.100	0.1000
55–58	0.155	0.156	0.1615	0.1565	0.1576	0.160	0.168	0.1562	0.1564
59–66	0.535	0.550	0.5092	0.5507	0.5222	0.522	0.584	0.54927	0.5443
67–70	0.480	0.390	0.4967	0.3922	0.4356	0.478	0.433	0.40966	0.4106
71–72	0.520	0.592	0.5619	0.5922	0.5971	0.591	0.520	0.56976	0.5717
Best weight (lb)	385.76	380.24	381.91	379.85	380.458	381.03	380.62	379.63	379.62
Mean weight (lb)	N/A	383.16	N/A	382.08	382.553	383.51	382.42	380.20	380.83
Standard deviation (lb)	N/A	3.66	N/A	1.912	1.221	1.92	1.38	0.41	0.61
Number of analyses	N/A	18,500	N/A	19,621	19,084	15,044	13,742	19,778	23,580

Table 18.11 Comparison of the optimization results obtained by CPA in the 120-bar dome problem

	Optimal cross-sectional areas (in2)							
	Case 1					Case 2		
Element group	HS [21]	RO [19]	CBO [23]	Present work	HS [21]	RO [19]	CBO [23]	Present work
1	3.295	3.128	3.1229	3.1229	3.296	3.084	3.0832	3.0831
2	3.396	3.357	3.3538	3.3538	2.789	3.360	3.3526	3.3526
3	3.874	4.114	4.1120	4.1120	3.872	4.093	4.0928	4.0928
4	2.571	2.783	2.7822	2.7822	2.570	2.762	2.7613	2.7613
5	1.150	0.775	0.7750	0.7750	1.149	1.593	1.5918	1.5923
6	3.331	3.302	3.3005	3.3005	3.331	3.294	3.2927	3.2928
7	2.784	2.453	2.4458	2.4458	2.781	2.434	2.4336	2.4336
Best weight (lb)	19707.77	19476.193	19454.7	19454.68	19893.34	20071.9	20064.5	20064.87
Average weight (lb)	–	–	19466.0	19454.72	–	–	20098.3	20064.93
Std (lb)	–	33.966	7.02	0.032	–	112.135	26.17	0.052
	Case 3					Case 4		
	RO [19]	CBO [23]	Present work	RO [19]		IRO [22]	CBO [23]	Present work
1	2.044	2.0660	1.9617	3.030		3.0252	3.0273	3.0250
2	15.665	15.9200	15.3594	14.806		14.8354	15.1724	14.6168
3	5.848	5.6785	5.8966	5.440		5.1139	5.2342	5.0201
4	2.290	2.2987	2.1967	3.124		3.1305	3.119	3.1404
5	9.001	9.0581	9.4318	8.021		8.4037	8.1038	8.5653
6	3.673	3.6365	3.5973	3.614		3.3315	3.4166	3.3648
7	1.971	1.9320	1.9498	2.487		2.4968	2.4918	2.4975
Best weight (lb)	31733.2	31724.1	31681.11	33317.8		33256.48	33286.3	33256.39
Average weight (lb)	–	32162.4	31701.56	–		–	33398.5	33281.73
Std (lb)	274.991	240.22	15.52	354.333		–	67.09	16.45

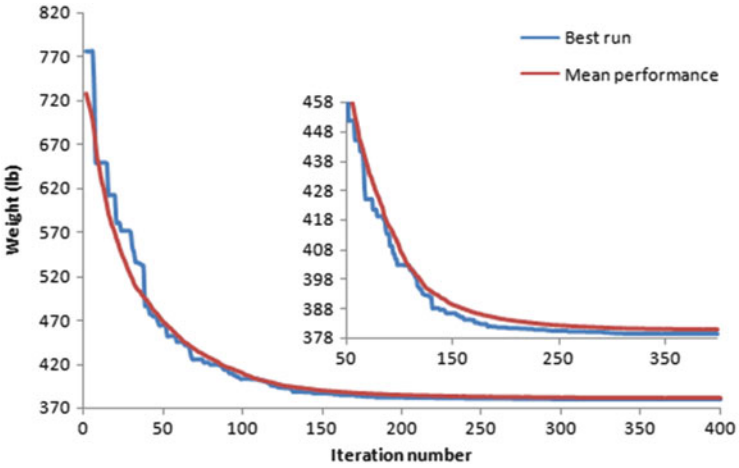

Fig. 18.15 Convergence curves for the best result and the mean performance of 20 independent runs for the 72-bar spatial truss

imposed on all nodes in x- and y-directions (Case 2), no stress constraints and displacement limitations of ± 0.1969 in (5 mm) imposed on all nodes in z direction (Case 3), and all the above mentioned constraints imposed together (Case 4). For Cases 1 and 2, the maximum cross-sectional area is taken as 5.0 in^2 (32.26 cm^2) while for Cases 3 and 4, it is taken as 20 in^2 (129.03 cm^2). The minimum cross-sectional area is taken as 0.775 in^2 (5 cm^2) for all cases.

Table 18.12 compares the results obtained by different optimization techniques for this example. It can be seen that CPA obtains the best results in Cases 1, 3, and 4 among the compared methods.

18.4.2.5 Design of a 200-Bar Planar Truss

A planar 200-bar truss as shown in Fig. 18.17 is optimized as the last test problem. The elastic modulus of the material is 30,000 ksi while density is 0.283 lb/in^3. The allowable stress for all members is 10 ksi (the same in tension and compression). No displacement constraints are included in the optimization process. The structure is divided into 29 groups of elements. The minimum cross-sectional area of all design variables is taken as 0.1 in^2. This truss is subjected to three independent loading conditions: (1) 1.0 kip acting in the positive x direction at nodes 1, 6, 15, 20, 29, 43, 48, 57, 62, and 71; (2) 10.0 kips acting in the negative y direction at nodes 1, 2, 3, 4, 5, 6, 8, 10, 12, 14, 15, 16, 17, 18, 19, 20, 22, 24,. . . , 71, 72, 73, 74, and 75; and (3) loading conditions 1 and 2 acting together. The members of the structure are linked together in 29 groups according to Table 18.12.

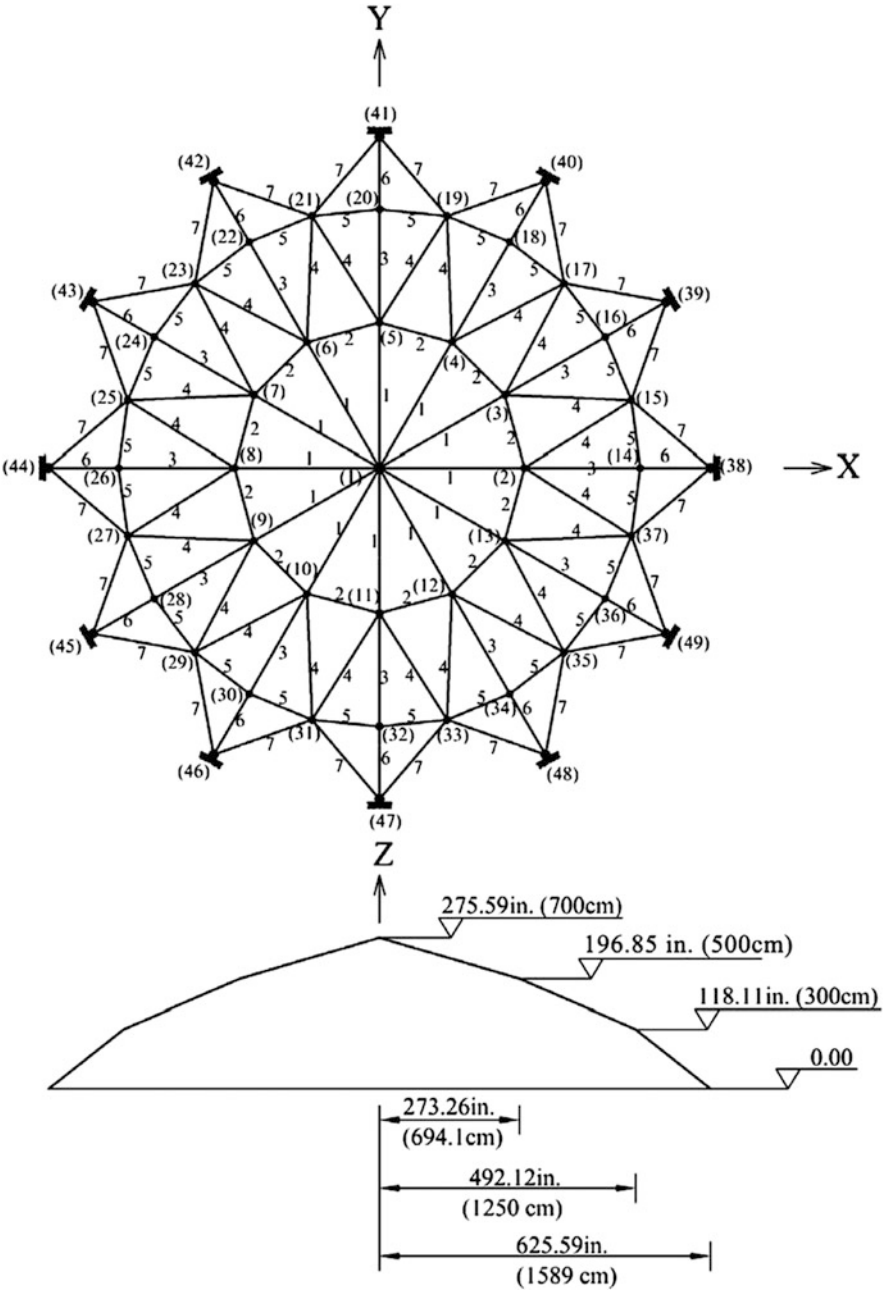

Fig. 18.16 Schematic of the 120-bar dome truss structure

Table 18.12 Comparison of optimization results obtained by CPA and other metaheuristic algorithms for the 200-bar truss problem

Element group	Members	Optimal cross-sectional areas (in^2)					
		CMLPSA [26]	SAHS [10]	TLBO [11]	HPSSO [27]	WEO [13]	Present method
1	1, 2, 3, 4	0.1468	0.1540	0.1460	0.1213	0.1144	0.1721
2	5, 8, 11, 14, 17	0.9400	0.9410	0.9410	0.9426	0.9443	0.9553
3	19, 20, 21, 22, 23, 24	0.1000	0.1000	0.1000	0.1220	0.1310	0.1000
4	18, 25, 56, 63, 94, 101, 132, 139, 170, 177	0.1000	0.1000	0.1010	0.1000	0.1016	0.1004
5	26, 29, 32, 35, 38	1.9400	1.9420	1.9410	2.0143	2.0353	1.9662
6	6, 7, 9, 10, 12, 13, 15, 16, 27, 28, 30, 31, 33, 34, 36, 37	0.2962	0.3010	0.2960	0.2800	0.3126	0.3055
7	39, 40, 41, 42	0.1000	0.1000	0.1000	0.1589	0.1679	0.1000
8	43, 46, 49, 52, 55	3.1042	3.1080	3.1210	3.0666	3.1541	3.1618
9	57, 58, 59, 60, 61, 62	0.1000	0.1000	0.1000	0.1002	0.1003	0.1152
10	64, 67, 70, 73, 76	4.1042	4.1060	4.1730	4.0418	4.1005	4.2405
11	44, 45, 47, 48, 50, 51, 53, 54, 65, 66, 68, 69, 71, 72, 74, 75	0.4034	0.4090	0.4010	0.4142	0.4350	0.4046
12	77, 78, 79, 80	0.1912	0.1910	0.1810	0.4852	0.1148	0.1000
13	81, 84, 87, 90, 93	5.4284	5.4280	5.4230	5.4196	5.3823	5.4132
14	95,96,97,98,99,100	0.1000	0.1000	0.1000	0.1000	0.1607	0.1545
15	102, 105, 108, 111, 114	6.4284	6.4270	6.4220	6.3749	6.4152	6.3976
16	82, 83, 85, 86, 88, 89, 91, 92, 103, 104, 106, 107, 109, 110, 112, 113	0.5734	0.5810	0.5710	0.6813	0.5629	0.5555
17	115, 116, 117, 118	0.1327	0.1510	0.1560	0.1576	0.4010	0.4425
18	119, 122, 125, 128, 131	7.9717	7.9730	7.9580	8.1447	7.9735	8.0928
19	133, 134, 135, 136, 137, 138	0.1000	0.1000	0.1000	0.1000	0.1092	0.1004
20	140, 143, 146, 149, 152	8.9717	8.9740	8.9580	9.0920	9.0155	8.9918
21	120, 121, 123, 124, 126, 127, 129, 130, 141, 142, 144, 145, 147, 148, 150, 151	0.7049	0.7190	0.7200	0.7462	0.8628	0.8925
22	153, 154, 155, 156	0.4196	0.4220	0.4780	0.2114	0.2220	0.2544

23	157, 160, 163, 166, 169	10.8636	10.8920	10.8970	10.9587	11.0254	11.1214
24	171, 172, 173, 174, 175, 176	0.1000	0.1000	0.1000	0.1000	0.1397	0.1000
25	178, 181, 184, 187, 190	11.8606	11.8870	11.8970	11.9832	12.0340	12.3304
26	158, 159, 161, 162, 164, 165, 167, 168, 179, 180, 182, 183, 185, 186, 188, 189	1.0339	1.0400	1.0800	0.9241	1.0043	1.0110
27	191, 192, 193, 194	6.6818	6.6460	6.4620	6.7676	6.5762	6.4103
28	195, 197, 198, 200	10.8113	10.8040	10.7990	10.9639	10.7265	10.5814
29	196, 199	13.8404	13.8700	13.9220	13.8186	13.9666	14.1288
Best Weight (lb)		25445.63	25491.9	25488.15	25698.85	25674.83	25651.58
Average weight (lb)		N/A	25610.2	25533.14	28386.72	26613.45	25957.15
Std (lb)		N/A	141.85	27.44	2403	702.80	254.06
No. of structural analyses		9650	19,670	28,059	14,406	19,410	34,560

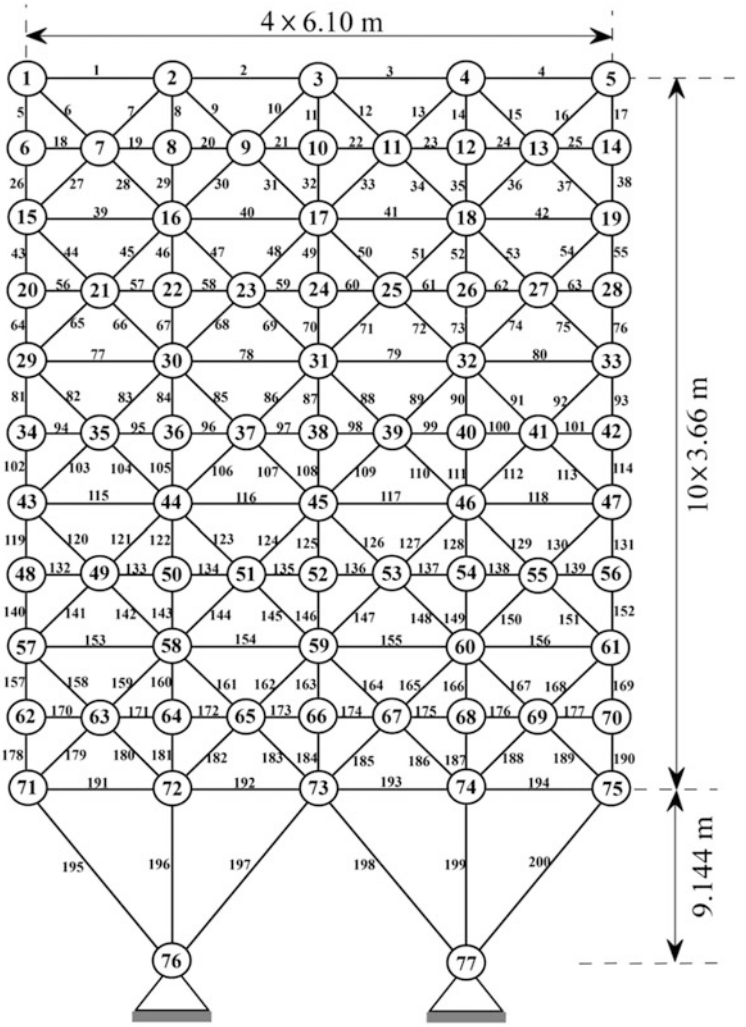

Fig. 18.17 Schematic of a 200-bar planar truss

Table 19.12 presents the optimum designs obtained by CPA, WEO [13], a Corrected Multi-Level and Multi-Point Simulated Annealing algorithm (CMLPSA) [26], SAHS [10], TLBO [11], and HPSSO [27]. Figure 18.18 shows the convergence curves for the best result and the mean performance of 50 independent runs for the 200-bar planar truss.

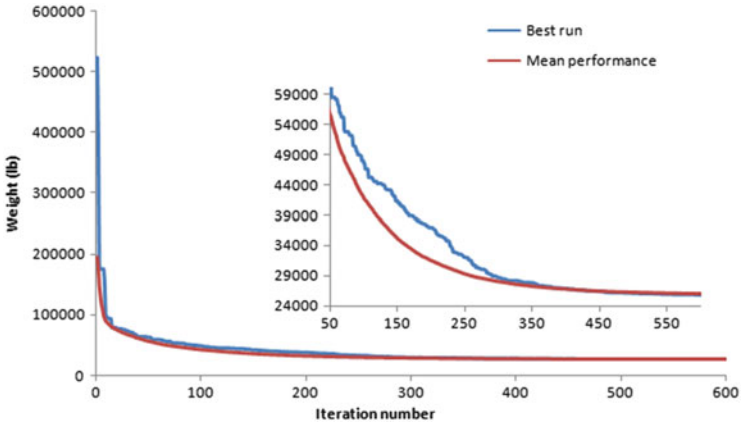

Fig. 18.18 Convergence curves for the best result and the mean performance of 50 independent runs for the 200-bar planar truss

18.5 Concluding Remarks

In this chapter a new population-based metaheuristic optimization method, namely, cyclical parthenogenesis algorithm (CPA), is presented. The algorithm is inspired by reproduction and social behavior of some zoological species like aphids, which alternate between sexual and asexual reproduction. CPA starts with a random population, considered as aphids, and iteratively improves the quality of solutions utilizing reproduction and displacement mechanisms.

Some mathematical and benchmark truss design problems are employed in order to investigate the viability of the proposed algorithm. Sensitivity of the proposed algorithm to its parameters is analyzed and the convergence behavior of the algorithm is studied using the diversity index. The results of the numerical examples indicate that the performance of the newly proposed algorithm is comparable to other state-of-the-art metaheuristic algorithms. CPA has found many interesting applications in design of structures, in particular in optimal design of truss structures with constraints as natural frequencies [28].

References

1. Kaveh A, Zolghadr A (2016) Cyclical parthenogenesis algorithm: a new metaheuristic algorithm. Adv Eng Softw (in press)
2. Piper R (2007) Extraordinary animals: an encyclopedia of curious and unusual animals. Greenwood Press, Westport, CT
3. Dixon AFG (1998) Aphid ecology: an optimization approach, 2nd edn. Blackie and Son, Glasgow
4. McGavin GC (1999) Bugs of the World. Blandford, London

5. Dawson KJ (1995) The advantage of asexual reproduction: when is it twofold? J Theor Bio 176 (3):341–347
6. Williams GC (1975) Sex and evolution. Princeton University Press, Princeton, NJ
7. Kaveh A, Zolghadr A (2014) Comparison of nine meta-heuristic algorithms for optimal design of truss structures with frequency constraints. Adv Eng Softw 76:9–30
8. Tsoulos IG (2008) Modifications of real code genetic algorithm for global optimization. Appl Math Comput 203:598–607
9. Sonmez M (2011) Artificial Bee Colony algorithm for optimization of truss structures. Appl Soft Comput 11:2406–2418
10. Degertekin SO (2012) Improved harmony search algorithms for sizing optimization of truss structures. Comput Struct 92–93:229–241
11. Degertekin SO, Hayalioglu MS (2013) Sizing truss structures using teaching-learning-based optimization. Comput Struct 119:177–188
12. Talatahari S, Kheirollahi M, Farahmandpour C, Gandomi AH (2013) A multi-stage particle swarm for optimum design of truss structures. Neural Comput Applic 23:1297–1309
13. Kaveh A, Bakhshpoori T (2016) Water evaporation optimization: a novel physically inspired optimization algorithm. Comput Struct 167:69–85
14. Li LJ, Huang ZB, Liu F, Wu QH (2007) A heuristic particle swarm optimizer for optimization of pin connected structures. Comput Struct 85:340–349
15. Camp CV (2007) Design of space trusses using Big Bang–Big Crunch optimization. ASCE J Struct Eng 133:999–1008
16. Erbatur F, Hasançebi O, Tütüncü I, Kiliç H (2000) Optimal design of planar and space structures with genetic algorithms. Comput Struct 75:209–224
17. Camp CV, Bichon J (2004) Design of space trusses using ant colony optimization. ASCE J Struct Eng 130:741–751
18. Perez RE, Behdinan K (2007) Particle swarm approach for structural design optimization. Comput Struct 85:1579–1588
19. Kaveh A, Khayatazad M (2012) A novel meta-heuristic method: ray optimization. Comput Struct 112–113:283–294
20. Soh CK, Yang J (1996) Fuzzy controlled genetic algorithm search for shape optimization. ASCE J Comput Civil Eng 10:143–150
21. Lee KS, Geem ZW (2004) A new structural optimization method based on the harmony search algorithm. Comput Struct 82:781–798
22. Kaveh A, Ilchi Ghazaan M, Bakhshpoori T (2013) An improved ray optimization algorithm for design of truss structures. Period Polytech Civil Eng 57:97–112
23. Kaveh A, Mahdavi VR (2014) Colliding bodies optimization: a novel meta-heuristic method. Comput Struct 139:18–27
24. American Institute of Steel Construction (AISC) (1989) Manual of steel construction allowable stress design, 9th edn. Chicago, Illinois
25. Saka MP (1990) Optimum design of pin-joined steel structures with practical application. ASCE J Struct Eng 116:2599–2620
26. Lamberti L (2008) An efficient simulated annealing algorithm for design optimization of truss structures. Comput Struct 86:1936–1953
27. Kaveh A, Bakhshpoori T, Afshari E (2014) An efficient hybrid particle swarm and swallow swarm optimization algorithm. Comput Struct 143:40–59
28. Kaveh A, Zolghadr A (2016) Cyclical parthenogenesis algorithm for shape and size optimization of truss structures with frequency constraints. Eng Optim (in press)